Polymer 50 (2009) 3508–3515

Contents lists available at ScienceDirect

Polymer

journal homepage: www.elsevier.com/locate/polymer

Magnetic core-bilayer shell nanoparticle: A novel vehicle for entrapment of poorly water-soluble drugs

Metha Rutnakornpituk*, Siraprapa Meerod, Boonjira Boontha, Uthai Wichai

Department of Chemistry and Center of Excellence for Innovation in Chemistry, Faculty of Science, Naresuan University, Phitsanulok 65000, Thailand

ARTICLE INFO

Article history:
Received 29 March 2009
Received in revised form
30 May 2009
Accepted 7 June 2009
Available online 12 June 2009

Keywords:
Magnetite
Nanoparticle
Bilayer

ABSTRACT

We are herein reporting a synthesis of indomethacin-loaded bilayer-surface magnetite nanoparticles and their releasing behavior. The particles were first stabilized with oleic acid as a primary surfactant, followed by poly(ethylene glycol) methyl ether-poly(ε-caprolactone) (mPEG–PCL) amphiphilic block copolymer as a secondary surfactant to form nanoparticles with hydrophobic inner shell and hydrophilic corona. mPEG–PCL copolymers with systematically varied molecular weights of each block (2000–2000, 2000–10,000, 5000–5000 and 5000–10,000 g/mol, respectively) were synthesized *via* a ring-opening polymerization of ε-caprolactone using mPEG as a macroinitiator. The particles were 9 nm in diameter and exhibited superparamagnetic behavior at room temperature with saturation magnetization (M_s) about 35 emu/g magnetite. Percent of magnetite and the copolymers in the complexes were determined *via* thermogravimetric analysis (TGA). The effect of mPEG and PCL block lengths in the copolymer–magnetite complex on the properties of the particles, e.g. particle size, magnetic properties, stability in water, drug entrapping and loading efficiency and its releasing behavior were investigated. This novel magnetic nanocomplex might be suitable for use as an efficient drug delivery vehicle with tunable drug-released properties.

1. Introduction

Water dispersible magnetic nanoparticles coated with water-soluble polymeric surfactants offer intriguing new opportunities for various biomedical applications such as magnetic resonance imaging (MRI) contrast enhancing agents [1–5], magnetic field-guided drug delivery [6,7], hyperthermia treatment of tumors [8] and biomolecular magnetic separation and diagnosis [9]. Especially in drug delivery applications, drug-loaded magnetic nanoparticles have been widely studied in an attempt to obtain the particles with high drug loading capacity, good stability in aqueous solutions, good biocompatibility with cells and tissue, desired releasing profile and retention of magnetic properties after modification with polymeric stabilizers [10–14]. Amongst these studies, therapeutic drugs were either physically adsorbed, chemically conjugated or ionically bound to the polymeric stabilizers [15]. Too low drug loading capacity is the major problem for these approaches. Formation of degradable microspheres loaded magnetic nanoparticles and therapeutic drugs has also been widely studied for uses in these applications [16–18]. Nonetheless, the magnetic response of the carriers is so low that it could not be effectively localized to a target area due to only a few percent of magnetic nanoparticles entrapped in the microspheres.

Many attemps have recently been made on preparing core/shell magnetite nanoparticles possessing polymer-coated surfaces [19–23]. Riffle et al. have recently reported the synthesis of poly(lactide-*b*-siloxane-*b*-lactide) triblock copolymers as magnetite nanoparticle stabilizers [24]. The siloxane central blocks functionalized with certain numbers of carboxylic acid were thought to anchor onto the particle surfaces and form polysiloxane inner shells, while polylactide tail blocks provided steric stabilization in hydrophobic carriers. Using the same concept, water dispersible nanoparticles were successfully achieved when triblock copolymers consisting of COOH-containing polyurethane central blocks and hydrophilic polyether tail blocks were used as dispersants [25,26]. In addition to ionic interaction, physical adsorption of amphiphilic molecules or polymers onto magnetite nanoparticle surface can efficiently yield water dispersible particles. Jain et al. have developed water dispersible magnetite nanoparticles stabilized with bilayer surfactants of oleic acid/Pluronic (poly(ethylene oxide)–poly(propylene oxide), PEO–PPO copolymer) and studied their loading efficiency and releasing behavior of anticancer agents [27]. It was hypothesized that PPO blocks were physically adsorbed onto the particle surfaces coated with oleic acid primary surfactant,

* Corresponding author. Tel.: +66 5596 3464; fax: +66 5596 1025.
E-mail address: methar@nu.ac.th (M. Rutnakornpituk).

0032-3861/$ – see front matter © 2009 Elsevier Ltd. All rights reserved.
doi:10.1016/j.polymer.2009.06.015

and PEO blocks provided steric stabilization in water. Similarly, fatty acids can also serve as both primary and secondary surfactants to produce bilayer-stabilized magnetite in aqueous fluids [28].

Our group has previously reported the synthesis of water dispersible magnetite nanoparticles having oleic acid and poly(ethylene glycol) methyl ether-poly(ε-caprolactone) (mPEG–PCL) amphiphilic diblock copolymer as polymeric stabilizers [29]. Hydrophobic PCL blocks hypothetically adsorbed onto magnetite nanoparticles coated with oleic acid primary surfactant, and hydrophilic mPEG blocks protruded outward from the particle surfaces to provide steric stabilization and dispersibility in aqueous fluids. The copolymers having $\overline{M_n}$ of 5000 g/mol mPEG-5000 g/mol PCL have been used as the stabilizer for this purpose.

The major objective of the present work is to study the effect of mPEG and PCL block lengths of the amphiphilic copolymer on structural and magnetic properties as well as their drug entrapping efficiency of the copolymer–magnetite complex. $\overline{M_n}$'s of mPEG and PCL were systematically varied to obtain relatively short and long block lengths of each component reflecting different degrees of hydrophobicity and hydrophilicity in the copolymer composition. It is envisioned that by tuning hydrophobic/hydrophilic ratio of the dispersant for magnetite nanoparticles, the competency for controlling their dispersibility and stability in water together with drug releasing behavior may be gained. In addition, the advantage of this work over the previously reported work using oleic acid/Pluronic surfactants [27] is the capability of tuning $\overline{M_n}$ of hydrolyzable PCL block to control its degradation rate, which thus essentially affects the releasing rate of any entrapped hydrophobic drug from the inner shell of the particles. In the current work, the influences of the copolymers composition on the particle size, stability in water, magnetic properties and drug releasing behavior were also studied.

2. Materials and methods

Unless stated otherwise, all reagents and solvents were used without further purification. Poly(ethylene glycol) monomethyl ether (mPEG) with $\overline{M_n}$ 2000 and 5000 g/mol (Acros) was dried in a vacuum oven at 60 °C under P_2O_5 for 48 h. ε-Caprolactone (ε-CL) (99%, Acros) was stirred over CaH_2 at room temperature overnight and distilled prior to use. Stannous octoate (95%, Sigma), iron (III) chloride anhydrous ($FeCl_3$) (Carlo Erba), iron (II) chloride tetrahydrate ($FeCl_2.4H_2O$) (Carlo Erba), ammonium hydroxide (J.T. Baker, 28–30%) and oleic acid (Fluka) were used as received. Cellulose dialysis tubing (Sigma-Aldrich) with molecular weight cutoff (MWCO) 12,400 was immersed in running water for 24 h before used.

2.1. Synthesis of mPEG–PCL copolymer

The synthesis method of mPEG–PCL diblock copolymers has been discussed in detail in our previous work [29]. Briefly, the copolymers were prepared through a ring-opening polymerization of ε-CL using an mPEG macroinitiator in the present of stannous octoate catalyst (Scheme 1). In the present work, $\overline{M_n}$'s of each block was systematically varied to obtain 2000–2000, 2000–10,000, 5000–5000 and 5000–10,000 g/mol, respectively.

2.2. Preparation of the copolymer-stabilized aqueous-based magnetite nanoparticles

$FeCl_3$ solution (1.66 g in 20 ml deionized water) and $FeCl_2 \cdot 4H_2O$ solution (1.00 g in 20 ml deionized water) were mixed together with stirring, followed by addition of 25% NH_4OH (20 ml). The dispersion was continuously stirred for another 30 min to complete the reaction. It was then centrifuged at 5000 rpm for 20 min to precipitate large aggregate and the aqueous supernatant was discarded. Oleic acid solution in hexane (2 ml in 20 ml hexane, 10%v/v) was then introduced into the magnetite dispersion with stirring. The dispersion was concentrated by evaporating hexane to obtain a black thick liquid of concentrated magnetite in hexane. Exact concentration of magnetite in the dispersion was determined *via* flame atomic absorption spectrometry (AAS). To prepare the copolymer-stabilized nanoparticles, 20 ml of the dispersion was

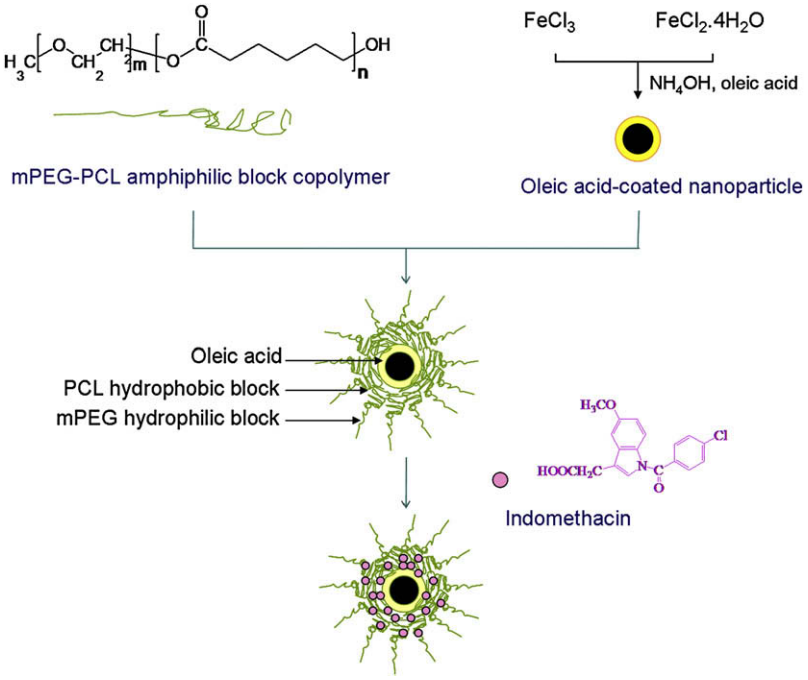

Scheme 1. Proposed entrapment mechanism of indomethacin in the hydrophobic inner-layer surfaces of the copolymer-stabilized magnetite nanoparticles.

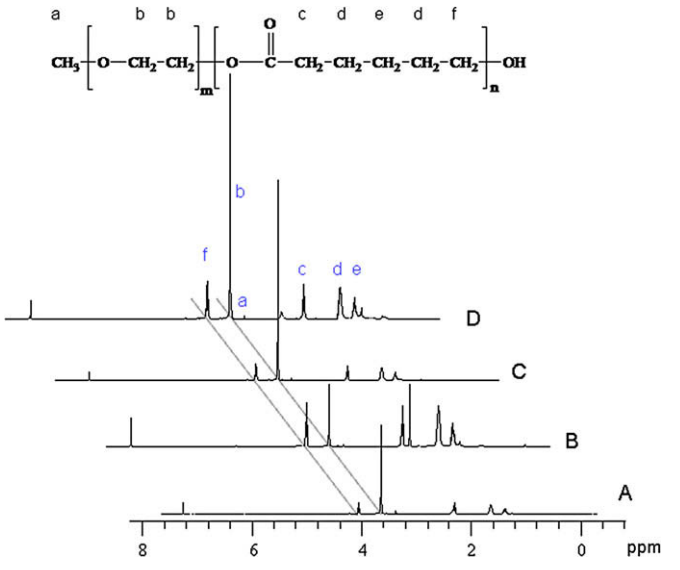

Fig. 1. ^{1}H NMR spectra of (A) 2000–2000 g/mol, (B) 2000–10,000 g/mol, (C) 5000–5000 g/mol, and (D) 5000–10,000 g/mol mPEG–PCL copolymers, respectively.

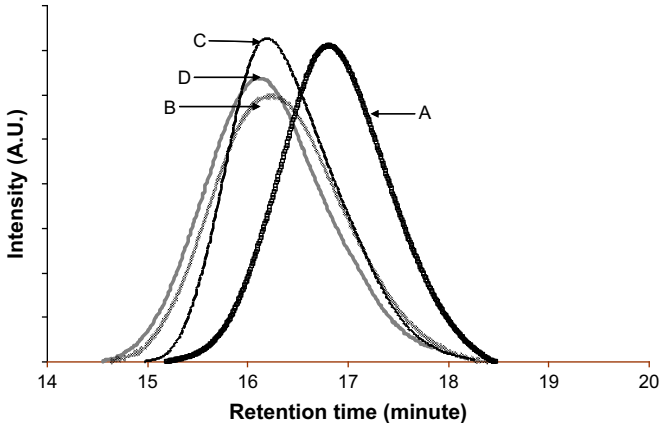

Fig. 2. GPC chromatograms showing the distribution of the molecular weights of (A) 2K–2K, (B) 2K–10K, (C) 5K–5K and (D) 5K–10K mPEG–PCL copolymers, respectively.

introduced into the copolymer solutions in deionized water (20 ml). The mixture was then sonicated for 4 h, followed by centrifugation at 3000 rpm for 20 min to remove large aggregate (Scheme 1). To prepare the copolymer-coated magnetite in a solid form for thermogravimetric analysis (TGA) and vibrating sample magnetometry (VSM), the aqueous dispersion was dialyzed against deionized water for 24 h and refreshed twice to remove the excess copolymer in the dispersion. The dispersion in the membrane was subsequently freeze-dried to obtain solid copolymer–magnetite complex.

2.3. Determination of $\overline{M_n}$'s of mPEG–PCL copolymers

^{1}H NMR was performed on a 400 MHz Bruker NMR spectrometer using $CDCl_3$ as a solvent. Gel permeation chromatography (GPC) data was conducted on PLgel 10 μm mixed B2 columns and a refractive index detector. Tetrahydrofuran (THF) was used as a solvent with a flow rate of 1 ml/min at 30 °C.

2.4. Characterization of magnetite nanoparticles

Magnetite concentrations in dispersions were analyzed *via* AAS and calculated from sample responses relative to those of standard and blank. Particles size and its distribution were observed from TEM technique. TEM images were taken using a Philips Tecnai 12 operated at 120 kV equipped with Gatan model 782 CCD camera. The samples were cast onto carbon-coated copper grids from aqueous dispersions. TGA was performed on SDTA 851 Mettler–Toledo at the temperature ranging between 25 and 600 °C at a heating rate of 20 °C/min under air atmosphere. Hydrodynamic diameter was measured by photocorrelation spectrophotometry (PCS) using NanoZS4700 nanoseries Malvern instrument. The sample dispersions were filtered and sonicated for 10 min before the measurement at 25 °C. Magnetic properties of the particles were measured at room temperature using a Standard 7403 Series, Lakeshore VSM. Magnetic moment of each sample was investigated over a range of ±10,000 G of applied magnetic fields using 30 min sweep time. Saturation magnetizations (M_s) were calculated using the concentration of iron measured by AAS and assuming that all irons were in the form of magnetite.

Table 1
$\overline{M_n}$ of mPEG–PCL block copolymers estimated from ^{1}H NMR and GPC techniques.

Copolymer	Copolymer name	Targeted $\overline{M_n}$ of each block (mPEG-ε-PCL)	Targeted $\overline{M_n}$[a] of the copolymer	$\overline{M_n}$[b]	$\overline{M_n}$[c]	PDI[c]
A	2K:2K	2000–2000	4000	4100	5400	1.71
B	2K:10K	2000–10,000	12,000	12,500	13,300	1.70
C	5K:5K	5000–5000	10,000	10,600	10,700	1.72
D	5K:10K	5000–10,000	15,000	15,400	14,400	1.72

[a] Calculated from the combination of the targeted $\overline{M_n}$'s of mPEG and ε-PCL blocks.
[b] Calculated from ($\overline{M_n}$ of mPEG + $\overline{M_n}$ of ε-PCL); $\overline{M_n}$ of ε-PCL estimated from ^{1}H NMR based on $\overline{M_n}$ of mPEG).
[c] $\overline{M_n}$ and polydispersity index (PDI) from GPC.

2.5. Investigation of indomethacin entrapment and loading efficiencies

To incorporate indomethacin to the copolymer–magnetite complex, the drug solution (2 ml, 25 mg/ml in THF) was added dropwise with stirring to an aqueous dispersion of the complexes (5 ml, 6.35% w/v of magnetite in water). The mixture was stirred for 30 min with heating to remove THF and to allow fully partitioning the drug into the hydrophobic shell surrounding the particles (Scheme 1). The excess drug precipitated out form the mixture and was removed by centrifugation at 3000 rpm. The drug-entrapped magnetite complexes were then magnetically separated from the dispersions to obtain the concentrated magnetite complexes swollen with water. Due to a good solubility of indomethacin in THF:ethanol solution (50:50%v/v), this solvent mixture was then

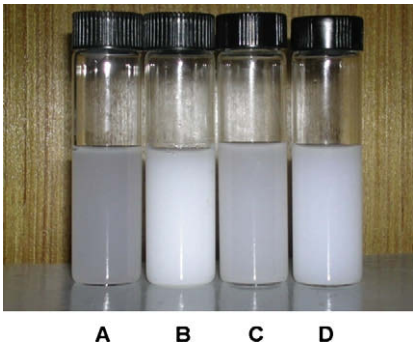

Fig. 3. Appearance of 1 wt % of (A) 2K–2K, (B) 2K–10K, (C) 5K–5K and (D) 5K–10K mPEG–PCL copolymers, respectively, in water.

Table 2
Effect of mPEG and PCL block lengths in the copolymer on transferring efficiency of the particles from hexane to water phases.

Type of copolymers used (mPEG–PCL)	Wt of Fe_3O_4 in feed (mg)	Wt of Fe_3O_4 in water phase (mg)	% Fe_3O_4 transferred to water phase[a]
2K:2K	29.4	23.2	78.9
2K:10K	29.4	23.2	78.9
5K:5K	29.4	26.9	91.2
5K:10K	29.4	24.4	83.0

[a] Calculated from (wt of Fe_3O_4 in feed) × 100/(wt of Fe_3O_4 dispersible in water phase).

added into the concentrated complexes to re-dissolve mPEG–PCL copolymers from the particle surfaces, resulting in the particle aggregation. After centrifugation to remove aggregated particles, the drug concentration in the supernatant, reflecting the amount of the entrapped drug in the complexes, was determined using UV–Visible spectrophotometer. Entrapment efficiency and drug loading efficiency were determined as following:

$$\text{Entrapment efficiency}\,(\%\,\text{EE}) = \frac{\text{Weight of drug in nanoparticles}}{\text{Weight of loaded drug}} \times 100$$

$$\text{Drug loading efficiency}\,(\%\,\text{DLE}) = \frac{\text{Weight of drug in nanoparticles}}{\text{Weight of nanoparticles}} \times 100$$

The indomethacin concentrations were determined using SPECORD S100 UV–Visible spectrophotometer (Analytikjena AG) coupled with a photo diode array detector. A standard curve at $\lambda_{max} = 320$ nm UV absorbance was established using identical conditions to calculate the amount of drug loaded on the particles [30,31]. Three different experiments were performed to obtain an average percent of each value.

2.6. In vitro releasing studies of entrapped indomethacin in the copolymer–magnetite complex

Indomethacin-loaded magnetite dispersions (5 ml) were introduced into a dialysis membrane bag immersed in a 300 ml-phosphate buffer solution releasing media (pH 7.4) and stirred at room temperature. At a predetermined time interval, 5 ml aliquots of the aqueous solution were withdrawn from the releasing media and 5 ml of phosphate buffer solution (pH 7.4) was replaced into the releasing media. Concentrations of the released indomathacin were determined *via* UV–Visible spectrophotometer at 320 nm wavelength.

3. Results and discussion

The aim of this work was to investigate the role of hydrophilic mPEG/hydrophobic PCL block lengths in the copolymer–magnetite complex on the properties of the particles such as particle size, stability in water, magnetic properties and indomethacin-entrapped and loading efficiency. The stabilizing mechanism of the particles in water was attributable to the physi-sorption of hydrophobic PCL central blocks to the particle surfaces pre-coated with oleic acid primary surfactant, while hydrophilic mPEG tail blocks provided steric repulsions in water. As a consequence, the particle surfaces possessed hydrophobic inner shells of oleic acid-PCL layers and hydrophilic corona of mPEG layers. Indomethacin, a poorly water-soluble model drug [32–34], was thus effectively entrapped into the inner hydrophobic shell. Owing to their high surface area to volume ratio of nanoparticles, it was envisioned that high drug loading efficiency should be gained. This system also enables for feasible tuning of $\overline{M_n}$'s of mPEG and PCL blocks to control the degree of hydrophilicity/hydrophobicity of the copolymers, which should affect dispesibility and stability of the particles in water.

3.1. Synthesis of mPEG–PCL copolymers with different block lengths

In-depth results and discussion on synthesis and characterization of the mPEG–PCL copolymer have been previously reported [29]. To control $\overline{M_n}$ of each block, molar ratios of OH groups at mPEG termini (macroinitiator) to ε-CL monomers were adjusted to obtain 2000 or 5000 g/mol mPEG blocks and 2000 or 10,000 g/mol PCL blocks. ^{1}H NMR was used to calculate $\overline{M_n}$'s of the copolymers by estimating $\overline{M_n}$'s of PCL blocks using the methylene protons adjacent to carbonyl groups in PCL repeating units (–(C=O)O–C$\underline{H}_2$–, 4.00 ppm, signal *f*) in conjunction with the methylene protons in the repeating units of mPEG (–$CH_2C\underline{H}_2O$–, 3.64 ppm, signal *b*) (Fig. 1). ^{1}H NMR spectra of the copolymers with various block lengths exhibited different integration ratios of signal *b* to signal *f*, which thus affected $\overline{M_n}$ of each block in the copolymers. The results

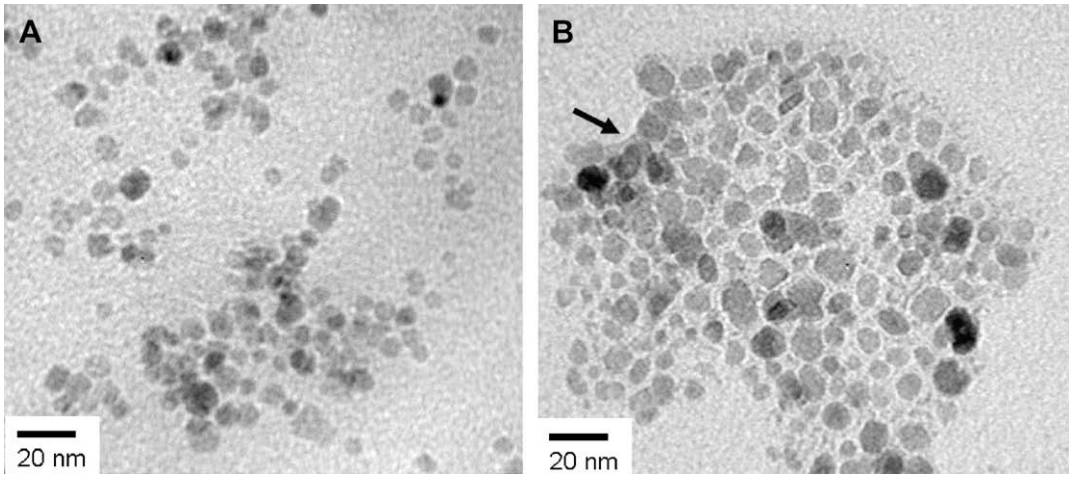

Fig. 4. TEM images of (A) copolymer-coated magnetite and (B) magnetite nanoparticles entrapped in copolymer micelles. The arrow in Fig. 4(B) indicated a polymeric thin film of the copolymer on the particles. Both TEM samples were directly cast from aqueous dispersions using 5K–5K mPEG–PCL copolymer dispersant.

Table 3
Hydrodynamic diameters of the copolymers and their complexes in aqueous dispersions.

Samples	Hydrodynamic diameter (nm)			
	(mPEG–PCL copolymer used)			
	(2K:2K)	(2K:10K)	(5K:5K)	(5K:10K)
Copolymer aqueous solution[a]	155.3 ± 1.6	181.5 ± 2.2	191.9 ± 1.2	203.1 ± 2.8
Copolymer–magnetite complex dispersion[b]	168.5 ± 1.3	195.3 ± 3.0	196.7 ± 1.7	218.5 ± 1.2
Drug-loaded copolymer–magnetite complex dispersion[c]	204.4 ± 1.5	213.3 ± 2.3	208.4 ± 1.4	236.2 ± 1.6

[a] The copolymer concentrations for PCS analyses were 0.1 mg/ml.
[b] The excess copolymers were removed by dialysis.
[c] The aggregated drug was removed by centrifugation.

exhibited reasonable correlation between the targeted $\overline{M_n}$'s and those estimated from ^{1}H NMR (Table 1). $\overline{M_n}$'s obtained from GPC also correlated well with those determined from ^{1}H NMR. It is interesting to point out that some transfer reaction might take place during the copolymerization reaction as indicated by the presence of extended tails of low $\overline{M_n}$ polymers in the GPC chromatograms (Fig. 2). Typical polydispersity indexes (PDI) of the copolymers ranged between 1.70 and 1.72 and the values were larger than those of the corresponding mPEG homopolymer (PDI = 1.09–1.10), indicating the formation of mPEG–PCL block structure.

Degree of solubility of the copolymers in water was highly dependent on $\overline{M_n}$ of hydrophobic PCL and hydrophilic mPEG, which in turn influenced the competence for stabilizing the particles in water. From the solubility test shown in Fig. 3, the copolymers having high $\overline{M_n}$ of PCL blocks (10,000 g/mol PCL of solution *B* and *D*) exhibited more opaque solutions, as compared to solutions *A* and *C*, indicating their poor solubility in water owing to hydrophobic nature of PCL blocks. Solution *B* showed the worst water solubility in the series due to its five-time difference in PCL/mPEG molecular weight ratio, while solution *A* exhibited the best solubility because of its comparable PCL and mPEG block length, combined with its relatively low $\overline{M_n}$.

3.2. Transferring efficiency of the particles from hexane to water phases

In our previous work, the detailed characterization of the mPEG–PCL-stabilized particles has been discussed [29]. FTIR was used to evidence the existence of the copolymers in the complexes. Also, the required concentrations of oleic acid and the copolymers to obtain eventual dispersions in water have been reported in the same paper. In the current work, we thus adopted those optimized conditions and focused on investigating the transferring efficiency of the particles from hexane to aqueous phases as a function of mPEG and PCL block lengths. Tuning the molecular weights of PCL and mPEG blocks in the copolymers is thought to influence dispersibility and stability of the particles in water. Namely, increasing $\overline{M_n}$ of PCL blocks can amplify degree of hydrophobicity of the copolymers, which consequently promotes their adsorbing competency to the oleic acid-pre-coated particles. On the other hand, increasing the block lengths of mPEG can enhance hydrophilicity of the copolymers, which accordingly promotes their dispersibility in water.

The transferring efficiencies were investigated *via* AAS by comparing the weight of magnetite dispersible in water phase with its loaded weight in hexane. According to the results in Table 2, the data support the premise that dispersibility of the particles in water was promoted by increasing mPEG block lengths and, in general, decreasing $\overline{M_n}$ of the PCL block. This enables for possible tuning their dispersibility in water by adjusting the ratio of hydrophilic to hydrophobic moieties in the copolymer composition. Percent of magnetite transferred to water phase ranged between 78.9 and 91.2% with the standard deviation ranging between 1.0 and 1.5%. The particles coated with 5K–5K mPEG–PCL copolymer showed the highest transferring efficiency in the series. This was attributed to its good solubility in water due to relatively long hydrophilic mPEG and short hydrophobic PCL blocks, which thus enhanced dispersibility of the particles in aqueous media.

3.3. Determination of the particle size and hydrodynamic diameters of the copolymers and their complexes

Fig. 4A illustrates a representative TEM image of the copolymer–magnetite complexes using 5K–5K mPEG–PCL dispersant deposited from an aqueous dispersion. The particles coated with other mPEG–PCL copolymers exhibited the same size and its distribution to those shown in Fig. 4A. Particle size of all samples ranged between 7 and 15 nm in diameter with the average of about 9 nm. It should be noted that oleic acid-coated magnetite also showed the same particle size, meaning that the particle size was not affected upon anchoring the copolymers onto the particle surfaces. The insignificant change of the particle size upon addition of the copolymers signified the thin coverage of the particles with the copolymers as indicated by the migration of the particles from hexane to water phases. In addition to individual particles coated with the polymeric surfactants, some nanoscale particle aggregations were also observed in TEM experiments (Fig. 4B). It was initially hypothesized that this aggregation belonged to the entrapment of the particles in the copolymer micelles.

PCS was thus conducted to investigate hydrodynamic diameter of the copolymer micelle and its distribution and also their complexes with the particles (Table 3). The results revealed that the micelle diameters of the copolymers ranged between 155 and 203 nm, depending on their molecular weights; higher molecular weights showed larger micelle sizes. It is known that micellar systems are dynamic, which always possesses micelles and unimers in equilibrium [35]. Shifting of the equilibrium between micelles and unimers allows for the formation of individually polymer-coated magnetite nanoparticles and magnetite-loaded micelles (Scheme 2).

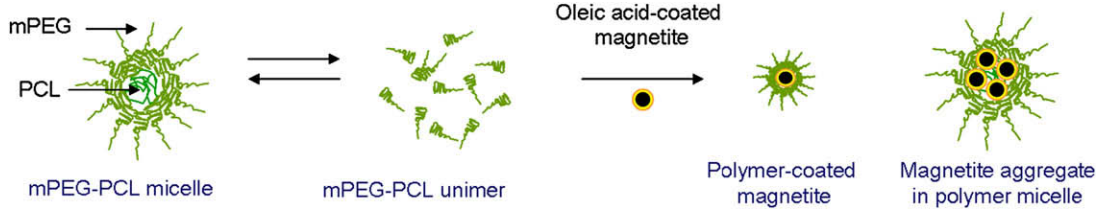

Scheme 2. Shifting of the equilibrium between micelles and unimers to the formation of polymer-coated magnetite and magnetite-loaded micelles.

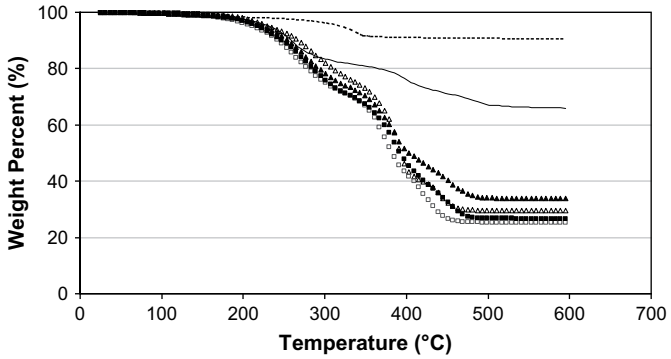

Fig. 5. TGA thermograms of bare magnetite (----), oleic acid-coated magnetite (——), magnetite coated with 2K–2K (△), 2K–10K (□), 5K–5K (▲), and 5K–10K (■) mPEG–PCL copolymers, respectively.

From the results in Table 3, hydrodynamic diameters of the magnetite–copolymer complexes in water increased as compared with those of the unloaded micelles due to the loading of the particles in the micelles [35–37]. The size of the magnetite–copolymer micelle complexes increased as the size of the copolymer micelles increased. According to TEM images, there were about 60–100 magnetite particles entrapped in the micellar cores. A polymeric thin film was apparent in the TEM image (Fig. 4B). The size of the complex increased when indomethacin was loaded and this was attributed to the encapsulation of indomethacin in the hydrophobic portion of the magnetite-entrapped micelles [38]. Determination of indomethacin entrapment efficiency, loading efficiency and its releasing behavior will be discussed in detail in Section 3.7.

3.4. Determination of the composition in the copolymer–magnetite complex

To determine the amount of oleic acid and the copolymer that can be associated to the particle surface, the copolymer–magnetite complexes were characterized to determine the mass loss *via* TGA in comparison with bare magnetite and magnetite coated with oleic acid (Fig. 5). Bare magnetite manifested weight loss between 270 and 350 °C with 91% char yield. This was attributable to the decomposition or desorption of the absorbed ammonium salt at elevated temperature and eventually loss some weight [39]. The weight loss of oleic acid-coated and the copolymer-coated magnetite were attributed to the decomposition of organic components

Table 4
Determination of the compositions in oleic acid-coated magnetite and copolymer–magnetite complexes.

	Char yield (%)[a]	Composition in the complexes (%)[d]		
		Fe_3O_4[b]	Oleic acid	Copolymer
Bare magnetite	91	100	—	—
Oleic acid-coated magnetite	66	73[c]	27[c]	—
Copolymer-coated magnetite (mPEG–PCL)				
2K:2K	30	33	12	55
2K:10K	25	28	10	62
5K:5K	33	36	13	51
5K:10K	27	29	11	60

[a] Assuming that char yield is the %wt of iron oxide completely oxidized at 600 °C.
[b] Assuming that all iron oxides are in the form of Fe_3O_4 at ambient temperature. %Fe_3O_4 is %char yield normalized with 0.91 factor (%char yield of bare magnetite).
[c] Ratio of Fe_3O_4 to oleic acid is 2.7:1 and this is used to calculate their ratio in other complexes.
[d] Total compositions of all components in the complexes are 100%.

Table 5
Concentrations of magnetite remaining dispersible in water after one month at 5 and 25 °C.

Type of copolymers used (mPEG–PCL)	% Fe_3O_4 remaining dispersible in water at	
	5 °C	25 °C
2K:2K	89	87
2K:10K	87	85
5K:5K	78	77
5K:10K	62	62

complexing to the particle surfaces. It should be noted once again that an excess of oleic acid and copolymers was removed from the dispersions using dialysis technique. TGA thermograms showed that the weight loss of oleic acid-coated magnetite ranged between 200 and 500 °C, while those of copolymer-coated magnetite ranged between 200 and 480 °C. It was assumed that % char yield of each sample shown in Table 3 was the weight of magnetite that was completely oxidized at 600 °C. Therefore, % char yield was thus normalized with 0.91 factor (% char yield of bare magnetite at 600 °C). To determine the amount of oleic acid in the complexes, the ratio of magnetite to oleic acid was determined (2.7:1, respectively), and this ratio was used to estimate % oleic acid in other complexes; hence, % copolymer in the complexes was calculated. According to the calculated percent of each component shown in Table 4, the complexes having higher $\overline{M_n}$ of PCL blocks (2K–10K and 5K–10K of mPEG–PCL, respectively) exhibited greater propensity in percent of copolymers in their compositions. This result supported the premise that high $\overline{M_n}$ of hydrophobic PCL block promoted their competency to complex onto the particle surfaces.

3.5. Stability of the copolymer–magnetite complex in water

Because the stabilizing mechanism of the complexes in water involved physi-sorption of hydrophobic PCL blocks to oleic acid-pre-coated magnetite surfaces, hence, their long-term stability in water was concerned. The dispersions were kept at 5 °C and 25 °C to investigate the effect of temperature on their stability in water. The dispersions were centrifuged (3000 rpm) after one month to precipitate unstable particles or aggregate that may arise and % Fe_3O_4 in the supernatant was analyzed *via* AAS technique. Table 5 shows final concentrations of the magnetites remaining dispersible in water after one month as compared to their initial concentrations. The dispersible magnetite concentrations ranged between 62 and 89%, regardless of the temperature of the dispersions. The high magnetite concentrations in water implied these complexes might

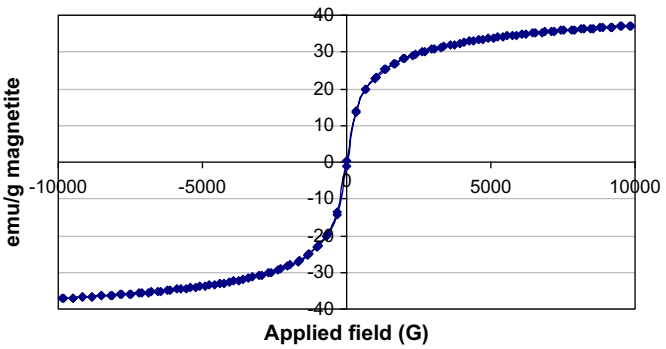

Fig. 6. A representative hysteresis curve of the copolymer–magnetite complex using 5K–5K mPEG–PCL dispersant, showing superparamagnetic behavior at room temperature.

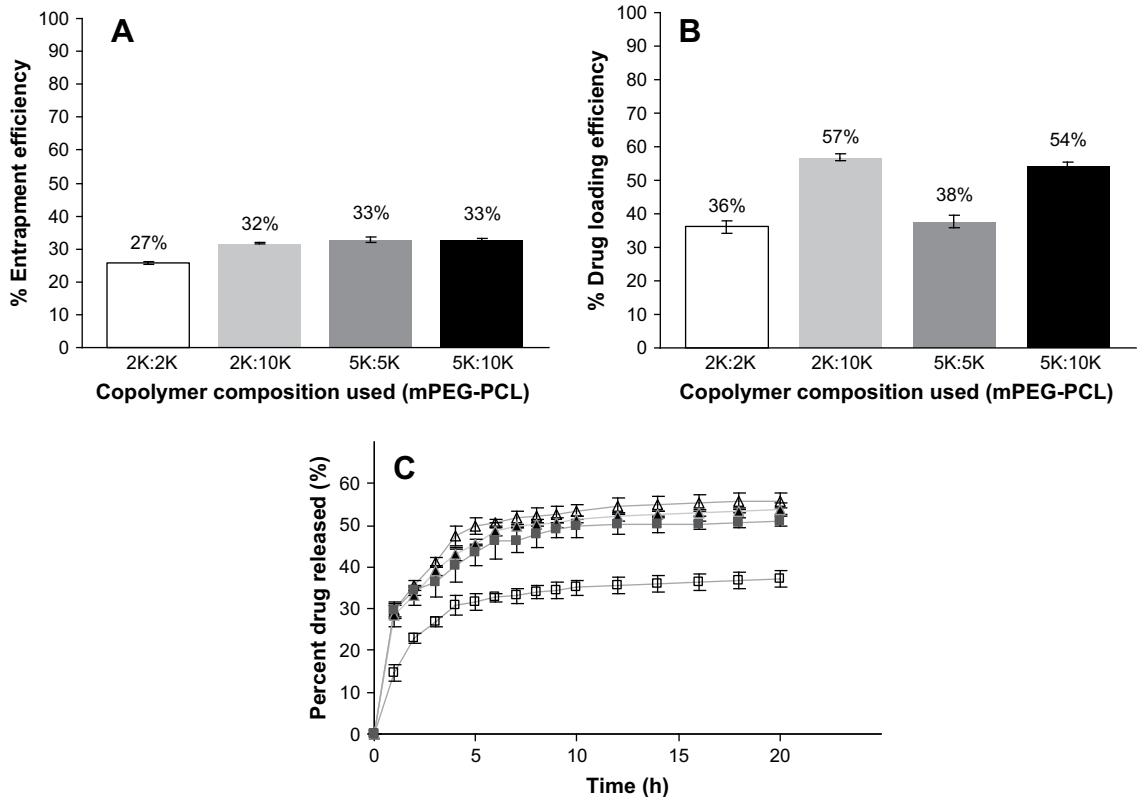

Fig. 7. (A) Percent entrapment efficiency (% EE), (B) percent drug loading efficiency (% DLE) and (C) indomethacin-released profile of the copolymer–magnetite complexes using 2K–2K (△), 2K–10K (□), 5K–5K (▲) and 5K–10K (■) mPEG–PCL copolymers, respectively.

be applicable for one-month uses. The partial aggregation of the particles in water was attributed to redissolution of the copolymer in the complex to the solution. The results also suggested that increasing $\overline{M_n}$ of the copolymers led to greater propensity for precipitation, probably owing to different degrees of dissolubility of each copolymer in water.

3.6. Magnetic properties of the copolymer–magnetite complex

A representative hysteresis curve of the copolymer–magnetite complex was illustrated in Fig. 6. They showed superparamagnetic behavior with saturation magnetization (M_s) at about 38 emu/g Fe_3O_4. Other complexes having different copolymer compositions or without copolymer also exhibited similar magnetic behavior and M_s values, indicating that the existence of the copolymers in the complexes did not affect magnetic properties of the particles.

3.7. Indomethacin entrapment efficiency, loading efficiency and its releasing behavior

In our previous report, we have presented a preliminary result of indomethacin entrapment efficiency and loading efficiency to confirm the formation of bilayer surfactant with a hydrophobic inner layer [29]. Indomethacin was selected as a model drug in the current studies due to its poor solubility in water. It was hence conceived that, once the hydrophobic indomethacin was added to the dispersion, it would somewhat partition to the inner hydrophobic shell (oleic acid–PCL layer) of the complex. Because THF was used in the encapsulation process of indomethacin, the residual THF that might be remaining in the dispersions was our concern for future uses in biomedical applications. Therefore, cytotoxicity testing of the drug-entrapped magnetite complexes was performed. According to our preliminary results, it was found that the dispersion was not toxic against Vero cell line up to 1% concentration of the sample (MTT assay method) (Supporting information). Detail studies regarding the toxicity of the magnetite complexes are warranted for future studies.

In the present report, the effects of mPEG and PCL block lengths in the copolymer on indomethacin entrapment efficiency (% EE), loading efficiency (% DLE) and its releasing behavior were studied. According to the results in Fig. 7A, % EE of indomethacin in these complexes was comparable to each other and the values were high up to 33% (33 mg indomethacin-entrapped/100 mg indomethacin-loaded). Considering the results in Fig. 7B, % DLE of these complexes ranging between 36 and 57% (360–570 μg/mg Fe_3O_4) were significantly higher than the previously reported number of % DLE in other bilayer nanomagnetic complexes (~6%) [27]. These impressive values thus suggested that indomethacin can be effectively entrapped in the copolymer–magnetite complex. This novel magnetic nanocomplex with bilayer-surface can hypothetically offer an efficient vehicle for loading any other poorly water-soluble drug in the formulation. It should be noted that % DLE in the complexes made of 2K–10K and 5K–10K mPEG–PCL copolymers were significantly higher than the other two. It was rationalized that high ratio of PLA block to mPEG block, reflecting high hydrophobic moiety, might influence the thickness of hydrophobic inner layer of the particle surfaces and subsequently promoted % DLE of the complex.

Percent release of indomethacin of all complexes reached their equilibrium within 12 h of dialysis (Fig. 7C). It was also observed that 57% or less of the drug was slowly released from the complex. Percent release of the drug in the case of 2K–10K copolymer-containing complexes (35%) was significantly lower than others (52–57%). This was attributed to the high degree of hydrophobicity in the copolymer (5 times of PCL to mPEG block length in the case of 2K–10K mPEG–PCL copolymer), resulting in the enhancement of binding affinity between indomethacin and the hydrophobic inner

shell (oleic acid-PCL layer) and thus suppressing indomethacin-released ability from the complexes.

4. Conclusions

Our interest has been to design water dispersible double-layer magnetite nanoparticles for effective entrapment of hydrophobic drugs. Magnetic nanocomplexes containing hydrophobic inner shell and hydrophilic corona have thus been synthesized. The particles were stabilized with oleic acid primary surfactant and mPEG–PCL block copolymer as a secondary surfactant. PCL was hypothesized to physically adsorb onto the particle surfaces pre-coated with oleic acid and mPEG hydrophilic blocks extended to water to provide steric stabilization. Dispersibility of the particles in water and the copolymer absorbability to the particle surfaces can be tuned by adjusting the ratio of $\overline{M_n}$ of hydrophilic mPEG to hydrophobic PCL. Namely, increasing $\overline{M_n}$ of mPEG blocks in the copolymers enhanced the particle dispersability in water, while increasing $\overline{M_n}$ of PCL blocks amplified their adsorbing competency to the hydrophobic inner layer of the particles. However, particle size and magnetic properties were not affected upon incorporating the copolymers in the complexes. In addition to individual particles coated with the polymeric surfactants, some nanoscale particle aggregation due to the entrapment of the particles in the copolymer micelles was also observed. The particles were stable in water with some aggregation observed after one month period. % EE of the complex was not dependent on the copolymer compositions, while % DLE and drug-released behavior highly depended on hydrophilic/hydrophobic ratio of the copolymer. This complex was hypothetically applicable to effectively load any other hydrophobic drugs by partitioning to the hydrophobic shell on the particle surfaces. These aqueous dispersions with tunable properties might be potentially used as magnetic field-directed drug delivery vehicles.

Acknowledgements

The authors thank the Thailand Research Fund (TRF) and Commission on Higher Education (CHE) (RMU4980006) for financial funding. The Center of Excellence for Innovation in Chemistry (PERCH-CIC), Commission on Higher Education, Ministry of Education is gratefully acknowledged for supports. The authors also thank Assist. Prof. Dr. Rakchart Traiphol for his suggestions regarding PCS results and Assoc. Prof. Dr. Sakchai Witaya-areekul for assistance in PCS technique.

Supplementary data

Supplementary data associated with this article can be found, in the online version, at doi:10.1016/j.polymer.2009.06.015.

References

[1] Kim DK, Mikhaylova M, Wang FH, Keht J, Bjelke B, Zhang Y, et al. Chem Mater 2003;15:4343–51.
[2] Gamarra LF, Brito GES, Pontuschka WM, Amaro E, Parma AHC, Goya GF. J Magn Magn Mater 2005;289:439–41.
[3] Jun YW, Huh YM, Choi JS, Lee JH, Song HT, Kim S, et al. J Am Chem Soc 2005;127:5732–3.
[4] Cheng FY, Su CH, Yang YS, Yeh CS, Tsai CY, Wu CL, et al. Biomaterials 2005;26:729–38.
[5] Lawaczeck R, Menzel M, Pietsch H. Appl Organomet Chem 2004;18:506–13.
[6] Asmatulu R, Zalich MA, Claus RO, Riffle JS. J Magn Magn Mater 2005;292:108–19.
[7] Tan ST, Wendorff JH, Pietzonka C, Jia ZH, Wang GQ. Chem Phys Chem 2005;6:1461–5.
[8] Roger J, Pons JN, Massart R, Halbreich A, Bacri JC. Eur Phys J Appl Phys 1999;5:321–5.
[9] Liberti PA, Rao CG, Terstappen LWMM. J Magn Magn Mater 2001;225:301–7.
[10] Sonvico F, Mornet S, Vasseur S, Dubernet C, Jaillard D, Degrouard J, et al. Bioconjugate Chem 2005;16:1181–8.
[11] Kohler N, Sun C, Wang J, Zhang M. Langmuir 2005;21:8858–64.
[12] Zhang JL, Srivastava RS, Misra RDK. Langmuir 2007;23:6342–51.
[13] Zhang Y, Zhang JJ. Colloid Interface Sci 2005;283:352–7.
[14] Hu F, Li Z, Tu C, Gao MJ. Colloid Interface Sci 2007;311:469–74.
[15] Pankhurst QA, Connolly J, Jones SK, Dobson JJ. Phys D Appl Phys 2003;36:167–81.
[16] Liu G, Yang H, Zhou J, Law SJ, Jiang Q, Yang G. Biomacromolecules 2005;6:1280–8.
[17] Eun HK, Yangkyu A, Hyo SL. J Alloys Compounds 2007;434–435:633–6.
[18] Michael DK, Yumei X, Carol JM, Martha RF, Haitao C, Axel JR. Eur J Pharm Sci 2008;35:96–103.
[19] Xie J, Xu C, Xu Z, Hou Y, Young KL, Wang SX, et al. Chem Mater 2006;18:5401–3.
[20] Yuan JJ, Armes SP, Takabayashi Y, Prassides K, Leite CAP, Galembeck F, et al. Langmuir 2006;22:10,989–93.
[21] Gomez-Lopera SA, Arias JL, Gallardo V, Delgado AV. Langmuir 2006;22:2816–21.
[22] Xianqiao L, Kaminski MD, Chen H, Torno M, Taylor L, Rosengart AJ. J Controlled Release 2007;119:52–8.
[23] Si S, Li CL, Wang X, Yu D, Peng Q, Li Y. Cryst Growth Des 2005;5(2):391–3.
[24] Ragheb RT, Riffle JS. Polymer 2008;49:5397–404.
[25] Zhang Q, Thomson MS, Carmichael-Baranauskas AY, Caba BL, Zalich MA, Lin YN, et al. Langmuir 2007;23:6927–36.
[26] Harris LA, Goff JD, Carmichael AY, Riffle JS, Harburn JJ, St. Pierre TG, et al. Chem Mater 2003;15:1367–77.
[27] Jain TK, Morales MA, Sahoo SK, Leslie-Pelecky DL, Labhasetwar V. Mol Pharmaceut 2005;2:194–205.
[28] Shen L, Stachowiak A, Fateen SEK, Laibinis PE, Hatton TA. Langmuir 2001;17:288–99.
[29] Meerod S, Tumcharern G, Wichai U, Rutnakornpituk M. Polymer 2008;49:3950–6.
[30] Kim SY, Shin IG, Lee YM, Cho CS, Sung YK. J Controlled Release 1998;51:13–22.
[31] Kim SY, Shin IG, Lee YM. Biomaterials 1999;20:1033–42.
[32] Park SJ, Lee YM, Hong SK. Colloids Surf B Biointerfaces 2006;47:211–5.
[33] Wei X, Suna N, Wu B, Yin C, Wu W. Int J Pharmaceut 2006;318:132–8.
[34] Zhang JX, Li XJ, Qiu LY, Li XH, Yan MQ, Jin Y, et al. J Controlled Release 2006;116:322–9.
[35] Talelli M, Rijcken CJF, Lammers T, Seevinck PR, Storm G, van Nostrum CF, et al. Langmuir 2009;25:2060–7.
[36] Yang X, Chen Y, Yuan R, Chen G, Blanco E, Gao J, et al. Polymer 2008;49:3477–85.
[37] Lecommandoux S, Sandre O, Checot F, Rodriguez-Hernandez J, Perzynski R. Adv Mater 2005;17:712–7.
[38] Shin IG, Kim SY, Lee YM, Cho CS, Sung YK. J Controlled Release 1998;51:1–11.
[39] Tao K, Dou H, Sun K. Chem Mater 2006;18:5273–8.